Workshop on Visualisation in Environmental Sciences (EnvirVis) (2024)
S. Dutta, K. Feige, K. Rink, and B. Nsonga (Editors)

Application, Adaption and Validation of the Thermal Urban Road Normalization Algorithm in a European City

Friedrich Striewski[1]*, Ennio Luigi Comi[2]*, Fiona Tiefenbacher[1]*, Natalie Lack[1], Mattia Battaglia[2], Susanne Bleisch[1]

1 FHNW University of Applied Sciences and Arts Northwestern Switzerland, Institute Geomatics
2 ZHAW Zurich University of Applied Sciences, Institute of Computational Physics (ICP)
∗ These authors contributed equally to this work.

Abstract

High resolution thermal infrared (TIR) remote sensing in the urban environment for building insulation inspection requires careful consideration of atmospheric and ground-located factors on the radiometric signal, with one being the microclimatic variability within the scene. Based on the assumption of roads as pseudo invariant objects, the TURN algorithm represents a tool to interpolate local temperature deviation within a scene and to normalize TIR-imagery in order to obtain a microclimate-free result. In this work we conduct adjustments, extensions and simplifications to the algorithm when applying it to a Middle-European urban environment. Based on research conducted in Aalen (Germany), we demonstrate our process of applying TURN for TIR-image normalization at high geometric resolutions and a scene composed of multiple adjacent flight-lines. Additionally, radiometric corrections to the TIR-image were applied prior to its processing by the algorithm. The corrections allow a validation of the TURN results by comparing them to ground-based reference data acquired during the flight with convincing agreement.

Categories and Subject Descriptors (according to ACM CCS): [100]Computing methodologies Modeling methodologies, [100]Applied computing Environmental sciences

1. Introduction

Recent trends in Land Surface Temperature (LST) estimation through Thermal Infrared (TIR) radiometry shift the focus away from low (>90 m) and medium-resolution images, acquired by satellite-based remote sensors, to high-resolution (<2 m) imagery from aerial systems, often deployed on planes, helicopters, or unmanned aerial vehicles (UAVs) [SSP*21]. With the increase of spatial resolution, a wide range of applications within the urban environment become feasible, from energy consumption estimation and modelling of cities [GCK17], assessment of urban heat island effects on the natural environment and human well being [ZXB*18], to planning, monitoring and management of "Smart Cities" [BMG19]. One fundamental factor that needs to be considered for calculations and interpretations of thermal signatures of single objects, as well as for their comparison across the scene, is local atmospheric variability, caused by insolation, precipitation, thermal storage capacity, humidity and wind on a scale of a few m^2 to km^2. [RHCH14] addresses such microclimatic effects with the development of the “Thermal Urban Road Normalization” (“TURN”) algorithm. By assuming street objects to be pseudo-invariant features, a continuous temperature-surface (“TURN-surface”) is interpolated from road temperatures. The TURN-surface is then used to “correct” the TIR scene for microclimatic influence and to derive a normalized, final image product. The original TURN algorithm by [RHCH14] showed promising results, but was developed and evaluated based on a single pilot site with distinct characteristics, like an overall flat relief in and around the urban area, which also featured an evenly distributed, grid-oriented road network. The algorithm was applied (i) to distinct, non-adjacent flight-lines processed individually and not covering the full city by a single scene or process, (ii) without environmental corrections, and (iii) with reference data from local weather stations, which [RHCH14] assesses as insufficient for accurate validation.

In the this work we adapt TURN to a Middle-European urban environment and assess potential adjustments to the calculation process. Based on a case study in Aalen, Germany, we apply TURN to a TIR-image of a four times higher geometric resolution (0.25 m) than used in the original study. In further contrast to [RHCH14], we use the algorithm i) over an entire city area with 5 adjacent flight-lines, ii) with the application of environmental corrections to the TIR-image prior to its processing by the algorithm, and (iii) with additional validation by temperature measurements acquired by a ground team during the flight.

Our focus also lays on the differentiation in the application of the algorithm. For one, we intend to use the normalization results to

DOI: 10.2312/envirvis.20241135

investigate the insulation standard of buildings across the flight perimeter as well as independently of the flight-line. Secondly, we intend to use the TURN-surface to detect heat and cold islands efficiently. In our case, it turned out that these two applications also require two slightly different calculation methods.
In the following sections, we first describe our study site and the specifics of data collection. Then, we briefly introduce the original TURN workflow by [RHCH14], before describing our adaptations to the methods and parameters used in the algorithm. Finally, we discuss our findings and validate the calculated results by comparing them with ground reference measurements.

2. Data Collection

2.1. Study area

The town of Aalen is located 70 km east of Stuttgart, Baden-Württemberg, Germany. Its height profile ranges from 450 to 500 m for most of the metropolitan area, while rural areas on the adjacent hills to the East and South reach heights up to 700m. About 21 km^2 of the city area were covered in 5 adjacent flight-lines between 8:15 to 9:15 p.m. on March 11 2023. Weather conditions during the day were cloudy skies with temperatures of up to 4 °C and slightly lower temperatures of -2 - 0 °C during the actual flight time. Relative humidity was around 85 %, with wind speed of up to 5 km/h, thus providing optimal conditions required for sufficient environmental contrast [Jen09]. The TIR-sensor used for the flight was an *ImageIR® 9400* thermal aerial camera with 0.03 °K radiometric accuracy in the 1.5 – 5.5 μm spectral region. Images were taken at a flight-height of approximately 1000 m above ground level and a ground sampling distance (GSD) of 0.25 m. Calculated from 1280 px x 1040 px frames, the final TIR image composite is a 26500 px x 12500 px raster in TIF-format. RGB orthophotos were ordered from the municipality in 0.20 m resolution and downsized to match the 0.25 m TIR image resolution. Flight planning data was acquired from the service provider tasked with conducting the flight. Road data was extracted from publicly available Open Street Map (OSM) data, which was filtered manually to include only primary and secondary asphalt roads.
Key differences of this research area and setup compared to the study area of Calgary, Canada used by [RHCH14] are summarized in Table 1:

Table 1: *Flight and TURN parameter comparison to [RHCH14].*

	Calgery (Canada)	Aalen (Germany)
Flight date & time	13th May 2012 0:00 – 4:30 a.m.	11th March 2023 7:45 - 10:15 p.m.
No. flight-lines direction	3, non-adjacent North-South	5, adjacent East-West
TIR Sensor (MWIR)	TABI-1800	ImageIR® 9400
Total area covered (km^2)	70	21
Geometric resolution (m)	1	0.25
Reference measurements	weather stations	iButtons & thermal cam.
Road mask noise correction	NDVI (vegetation) histogram (cars)	Smoothing and pixel binning
Road mask ref. temperature	mode	geometric mean

2.2. Terrestrial Reference Measurements

Thermal cameras record infrared radiance of a usually ground-based source, whose radiative energy depends on its (true) kinetic energy, its emissivity as well as distortional effects of surface and the atmosphere temperature between sensor and object [BMG19]. During the flight, a ground team was taking reference measurements on several sites across the city of Aalen. A combined approach of manual and automatic readings was chosen: With East-West flight direction, manual readings were taken from a main road ("Richard-Wagner Strasse"), intersecting flight-lines 2-4 in North-South direction. The road used has an inclination of 2.6 ° towards the north, with the southern-most sample point being located 14 meter of elevation lower than the northern-most point. Using a “FLIR” handheld thermal camera, three sets of readings, in approx. 30 min intervals, were taken at 18 sample locations across the 300 m long profile during the flight. More details about the reference measurements and locations of the sample points can be found in the supplementary information.
Small-sized thermal data loggers called “iButtons” from Maxim Integrated Products Inc., have frequently been applied in microclimate research as a low cost, low maintenance solution for the recording of (ground) temperatures (see [MDH*21] for examples). A total of 9 DS1922L-F5# and DS1921G-F5# iButton temperature loggers, with a nominal accuracy of 0.5 °C in the -40 °C to +85 °C temperature range, were placed in water, fields, on buildings and asphalt and set to one reading per 600 s interval. Relevant for this study are the two temperature loggers placed on asphalt in the "Richard-Wagner Strasse" and near "Weilerstrasse".

3. Methodology

The TURN algorithm as developed by [RHCH14] consists of the following five major processing steps: 1) Extraction of a road mask, cleaning of noise originating from sources like vegetation, parked vehicles, and construction sites. 2) Point sampling of a single road point per interval, using an auxiliary grid with predefined width (e.g., a cell size of 20 m x 20 m). A sample point represents the *median* temperature of all road pixels within this cell. 3) Calculation of a mode deviation per sample point by subtracting the most "road-like" temperature of the entire road mask for a given flight-line from the median temperature, determined in the previous step. 4) IDW (Inverse Distance Weighted) interpolation of a "TURN-surface" from the sample points, which represents and visualises microclimate characteristics across the scene. 5) Normalization of radiant temperatures, by subtracting the TURN-surface from the original TIR-image on a pixel-by-pixel basis.
To verify the normalization of the algorithm, the authors of the original study calculate the RMSE (Root Mean Squared Error) on the road mask between the normalized TIR and the most "road-like" temperature of the entire flight-line. TURN output consists of (i) the normalized thermal image, (ii) the TURN-surface as an indicator for microclimate variability, and (iii) the RMSE value per flight-line, used to assess the quality of the chosen parameters in the process.
For our study we followed the steps of TURN as outlined above with several adjustments which will be described in detail in sections 3.1 - 3.6.

3.1. Thermal Infrared Image Correction

A quantitative analysis of ground object temperatures measured through TIR-images requires a careful calibration for factors such as the emissivity of materials (e.g. roofing or road materials), scene morphology (e.g. relief and housing density, influencing sky visibility) as well as atmospheric influences [BMG19]. [RHCH14] note that missing or insufficient TIR-image corrections, prior to its use in TURN, can limit the validity of the algorithm's output.
When evaluating the raw IR data, we noticed deviations from our reference measurements on highly emissive materials in the range of 5 to 10 K, which could be expected from the results of [MC16]. Consequently, extensive corrections of the data and quantification of the influences of the atmosphere, emissivity, sky visibility and camera sensor and lens were necessary. To estimate the transmission of the atmosphere in our relevant wavelength range, the "Modtran" demo from Spectral Sciences Inc. [SPE] was used, with the "Mid-latitude winter atmospheric model" parameter selected as most fitting preset for our sampling date and location. A humidity and temperature sensor was attached to the aircraft to monitor the values during the flight, take-off and landing in order to incorporate them into the calculations of the upwelling radiance.
The sky-view factor (SVF) is a measure of how much of the reflected IR-radiation from an object comes from the (cold) sky and how much comes from warmer surroundings. As a *local* factor, it has a pixel-by-pixel influence on the TIR-mosaic. The SVF was calculated using a DSM (Digital Surface Model), while sky temperatures (downwelling radiance in the Midwave Infrared (MWIR) region) during flight times were estimated using a space blanket.
For this study, only the emissivity of construction asphalt for the road mask was required, which we extracted from the "Ecostress Spectral Library" [NAS] in the MWIR range. After extensive parameter evaluations, considering various reference temperature points in the flight-perimeter and consultation with the camera manufacturer, we had to add a sensor deviation (or lens distortion) of approximately 2 K, to get as close as possible to the measured reference temperatures over the entire area. As the TURN algorithm solely requires road temperatures to calculate microclimatic influences, asphalt emissivity, transmission and camera/lens influences could be corrected *globally* on the TIR mosaic.

3.2. Calculation of Road Mask

For the extraction of a road mask, public data from Open Street Map (OSM) was used, with any objects other than primary and secondary asphalt roads manually filtered out. Despite having smaller road diameters compared to the research site of [RHCH14], a similar 1.5 m buffer around the road axis was chosen, in order to obtain sufficient samples and allow comparisons between studies. The cleaning for noise stemming from vegetation and temperature outliers (parked vehicles on narrow roads, construction sites) had to be approached differently: As RGB-NIR data was not available, the NDVI could not be calculated as done by [RHCH14]. Masking vegetation based on the green channel of the RGB alone, which depicts summer conditions with lush canopy in contrast to the actual winter conditions encountered during TIR acquisition, resulted in too much data loss to be of use.
To reduce the influence of outliers on the TURN calculations, the TIR-mosaic used for the calculation of the road mask was reduced from a resolution of 0.25 m/px to 1 m/px and a Gaussian smoothing filter was applied (see supplementary information). This led to a smoothing of temperature spikes from cars and vegetation in both directions, while the decisive average road temperature is marginally distorted. While such a "polished" 1 m TIR-mosaic was used for the calculation of the interpolated TURN-surface, the original TIR mosaic with 0.25 m resolution was used for the final normalization. Such outliers can appear when a grid cell (see section 3.3) contains only a small part of a road that might have a car in it or is full of vegetation.

3.3. Sampling of Road Temperature Median

[RHCH14] identifies spectrally similar and adjacent pixels as a challenge for interpolation, proposing a reduction technique: First, the perimeter of a flight-line is divided into a regular grid. Then, the median temperature road pixel per grid cell ("tile") is determined, using this value as representative of the tile and as basis for the interpolation. While we see no reason why a *mean* value should not be calculated instead, we too used the *median* value, in order to stay as close as possible to the original algorithm. The temperature representative needs to be associated with a certain position (pixel) within the tile. Ideally, the median or the pixel closest to the mean is sought and the point is placed exactly there. However, this is associated with increased computational effort, depending on the sizes of the grid and flight-perimeter. A simpler option for placing the pixel, chosen by us, is the *random* placement within a tile, but on the street mask. This alternative approach results in a maximum position error of the tile length multiplied by $\sqrt{2}$. However, as the tile size should be chosen so that the road mask does not show enormous deviations, this error should have a minor influence on the outcome. An illustration of the road mask with a regular grid and the median temperature road pixel can be found in the supplementary material.
Regarding the tile size, for 1 m TIR resolution, good results according to [RHCH14] were established with a 20x20 m grid and the location of the median pixel at its actual location on the road mask. In our instance, we evaluated different tile sizes (5x5, 15x15, 20x20 and 30x30 m) with the random placement of the representative pixel and compared the resulting RMSE. It turned out that the RMSE decreases for smaller tile sizes, as it has been reported by [RHCH14] as well. This can be explained by the more intensive averaging of pixel values or a potential shift of the median taking place with larger tiles. For this reason, and to reduce computational demand, we decided to use a tile size of 15x15 m for further calculations. The resulting representative points for a 15x15 m grid, colored per flight-line, are shown in Figure 1.
As an additional step, [RHCH14] apply a smoothing technique for the uneven edges of a flight-line, consisting of null values, by detecting the edges with a Laplacian edge detection filter, adding additional border samples with values from the nearest road sample and finally cleaning excess data within the grid cell to prevent over-sampling. Adjacent flight-lines reduce the overall amount of smoothing and shift the problem to the edges of the perimeter. As a simpler alternative to the workflow above, we suggest reducing the perimeter within the bounds of the TIR area. While there is some

data loss, each grid tile is calculated homogeneously without any distortional effects at the edges.

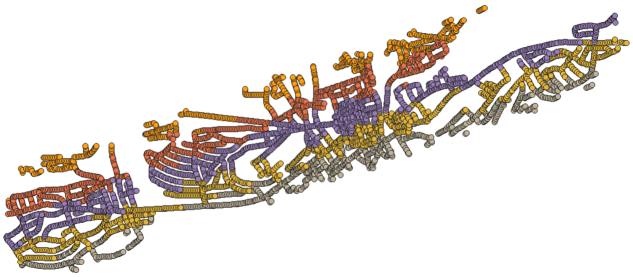

Figure 1: *Sampled temperature representatives (support points for the interpolation) colored per flight-line. Flights were conducted in West-East direction from North (flight-line 1, orange) to South (flight-line 5, grey).*

3.4. Representative Road Temperature

Based on the premise that roads act as pseudo-invariant features and that the road mask has been cleaned of noise, any deviation from the mode temperature of the road mask is assumed to be related to microclimatic effects [RHCH14]. For non-adjacent flight-lines, [RHCH14] identifies the *mode temperature* of the road mask (per flight-line) as the most "road-like" temperature, which is subsequently used as a subtrahend to calculate the mode deviation per temperature representative (see section 3.3) across the flight-line:

$$\delta_{ij} = (T_{ij} - T_{mode}) \tag{1}$$

Where,
δ_{ij} = Deviation from mode at pixel (i, j)
T_{ij} = Temperature of pixel (i, j)
T_{mode} = Road temperature mode for a given flight-line

Initial results from TURN calculations on the "Aalen" dataset indicated that the mode value might not be the ideal indicator for the most "road-like" temperature approximation. An example from this specific dataset would be the warm city center, which is located to a large extent in the second flight-line and features a high number of equally warm pixels. Based on these findings, we calculated the *geometric mean* temperature of the road mask per flight-line and used it as a subtrahend in the deviation calculation instead:

$$\delta_{ij} = (T_{ij} - T_{gmean}) \tag{2}$$

Where,
δ_{ij} = Deviation from the geometric mean at pixel (i, j)
T_{ij} = Temperature of pixel (i, j)
T_{gmean} = Geometric mean of road temperatures for a given flight-line (most "road-like" temperature)

Subtracting the geometric mean from the median temperature results in values that well represent the microclimate inside a single flight-line, when interpolated to a TURN-surface (see section 3.5). In contrast to the original study, our scene is, however, assembled from multiple adjacent flight-lines, which requires a second consideration: If there are significant differences in the geometric mean *between* flight-lines, e.g., as caused by temperature drift during the flight, using the geometric mean per flight-line may prove problematic when aiming to compare objects across the *entire perimeter*, as it is required by our research focus in building insulation inspection.
Adjacent flight-lines require overlap and repeated passes over the same ground area due to necessary flight manoeuvres. Infrared signals in the assembled TIR-mosaic can thus represent a blend of frames, sampled at close, but different flight times. This blend of frames can lead to a beneficial averaging between flight-lines to counteract a possible temperature drift during flight time. Nevertheless, we wanted to include a possible temperature drift during the flight time, as our reference measurements suggested, and therefore calculated the geometric mean temperature of the entire road mask for the entire flight perimeter. The deviation from the grid tile median values is thus calculated as follows:

$$\delta_{ij} = (T_{ij} - \overline{T}_{gmean}) \tag{3}$$

Where,
δ_{ij} = Deviation from the geometric mean at pixel (i, j)
T_{ij} = Temperature of pixel (i, j)
$\overline{T}_{gmean}$ = Geometric mean of all road temperatures of all flight-lines (most "road-like" temperature)

3.5. Interpolation and Normalization

Deviation values calculated in section 3.4 are interpolated over the entire perimeter to calculate the TURN-surface, which represents the microclimatic influence on the originally measured temperatures. According to [RHCH14], inverse distance weighting (IDW) is the most suitable interpolation method for TURN-surfaces. For computation we use the OSGeo/GDAL library in version 3.7.1 [GDA]. Several parameters can influence the resulting interpolation. We highlight a few in section 4.3. In the supplementary material we show a comprehensive IDW-parameter study and the influence on RMSE as well as the resulting TURN-surfaces. For parameters not explicitly mentioned by us, the default parameters of the library apply.
For temperature normalization, we follow the process of [RHCH14] by subtracting the interpolated TURN-surface from the corrected TIR-mosaic, following equation 4 and calculate a microclimate corrected TIR-mosaic as final output of the algorithm.

$$N_{ij} = (T_{ij} - \delta_{ij}) \tag{4}$$

Where,
N_{ij} = Normalized radiant temperature of pixel (i, j)
δ_{ij} = Deviation from pixel (i, j)
T_{ij} = Original radiant temperature of pixel (i, j)

3.6. Validation and parameter optimization with RMSE

The goal of the normalization is that the final road temperatures are as close as possible to the most "road-like" temperature of the roads in a flight-line (T_{gmean}) or, if desired, of all the roads in the entire perimeter ($\overline{T}_{gmean}$). To quantify the efficiency of the normalization, [RHCH14] calculate the RMSE between the most "road-like" temperature and the TIR road temperature before and after the application of TURN. We implemented this step similarly with randomly distributed test pixels on the road mask and calculated the RMSE as follows (here shown for a given flight-line):

$$RMSE = \sqrt{\frac{\sum_1^n (T_{gmean} - T_{Rij})^2}{n}} \tag{5}$$

Where,
T_{gmean} = Geometric mean of road temperatures of a given flight-line (most "road-like" temperature)
T_{Rij} = TIR Road temperature before or after TURN at test pixel (i, j)
n = Number of total test pixels

A decrease in RMSE values after normalization indicates less variability between road temperatures and the representative temperature per flight-line, and consequently an effective reduction of the local microclimatic impact on the TIR-mosaic. The quality of TURN normalization as well as the effect of the chosen interpolation parameters can be measured by the percentage of decrease between normalized and not normalized RMSE and is shown in equation 6.

$$RMSE_{decrease}(\%) = \frac{RMSE_{unnorm.} - RMSE_{norm.}}{RMSE_{unnorm.}} * 100 \tag{6}$$

Where,
$RMSE_{unnorm.}$ = RMSE before normalization
$RMSE_{norm.}$ = RMSE after normalization

4. Results & Discussion

In this work, we applied the TURN algorithm developed by [RHCH14] to a European city with the overall aim of detecting microclimate variability at the time of flight and analyzing building insulation standards. In this section, we would first like to draw attention to the differences between our and the originally published method as well as their impact on the results, then take a closer look at the influence of various interpolation parameters and finally validate our results with reference measurement data. In addition, we investigate the correlation between the TURN-surface and building area on the one hand, and the sky-view factor on the other.

4.1. Image Resolution and Adjacent Flight-Lines

With a flight height at around 1000 m above ground level, we achieved a resolution of 0.25 m per pixel in our TIR-mosaic. In our opinion, a resolution of this magnitude is an advantage when investigating buildings as it allows to remove unnecessary building parts without losing a large quantity of the building envelope. While we hoped to make a statement about high IR-resolution for the evaluation of the microclimate, we were forced by the absence of the NIR-channel in the RGB-image to perform a down-sampling in order to minimize the influences of vegetation and vehicles on the road mask. As a higher geometric resolution leads to more detail, in e.g. vegetation, it also requires a better removal of those disturbances.
A significant difference to the original study is that we do not consider individual flight-lines, but calculate the TURN algorithm with five contiguous flight-lines. This is particularly important when the representative temperature per flight-line is calculated and the deviation from the median temperature pixel is then interpolated across flight-lines. If the representative temperature of the flight-lines differs significantly, for example due to a drop in temperature during the flight, this will become apparent when interpolating the TURN-surface at the edges of the flight-lines. For this reason, it is even more important for contiguous flight-lines that the representative temperature of the flight-line is well chosen. In our case, a mean value to calculate the representative temperature of the flight-lines rendered better results for microclimate analysis with smoother interpolation across flight-lines compared to the mode value. An important aspect is that the mode only represents the most "road-like" temperature well if it is also represented by a sufficiently high count of values. If several different values are present in similarly high counts, then the mode value should not be used.

4.2. TURN for Microclimate and Building Insulation Inspection

One advantage of taking TIR-images from a remote sensing aircraft is that images of large areas can be taken within a short time and in relatively high quality. This allows efficient temperature data evaluation for a large number of buildings. The microclimate plays a major role in the evaluation of the insulation standard and cross-area comparison between the buildings. The TURN algorithm is intended to prevent a well-insulated building in a heat island from being rated worse than a poorly insulated building in a cold island. The microclimate raster is created with the TURN-surface and can be of additional interest for urban planning. The question here is to what extent heat islands that are detected during winter months are also present in summer. A study in a Chinese city suggests that heat and cold islands behave very similarly in summer and winter [YYZ20].

Our analysis of the TIR-mosaic and the reference measurements suggests that the flight probably started a few minutes too early in the evening, with the first flight-line and the asphalt roads still in the process of cooling down. If this had not been the case, we would not have had to distinguish between $\overline{T}_{gmean}$ and T_{gmean} to obtain a microclimate map.
The difference between the TURN-surface calculation with $\overline{T}_{gmean}$ and T_{gmean} can be seen in Figure 2. If T_{gmean} is used for each individual flight-line (Figure 2 **B**), then the temperature deviation also refers to the representative temperature of the flight-line. It is subsequently interpolated between the flight-lines and the result is a raster that illustrates the microclimate vividly, but could have interpolation issues near flight-line intersections. However, if $\overline{T}_{gmean}$ of the whole perimeter is used (Figure 2 **A**), then the temporal de-

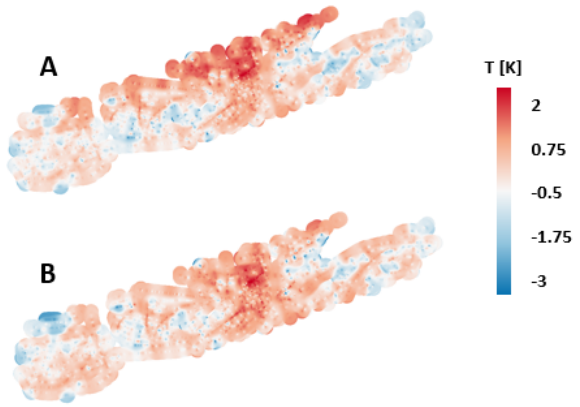

Figure 2: *TURN-surfaces calculated with $\overline{T}_{gmean}$ (A) and T_{gmean} (B).*

pendency, i.e. cooling, from the first flight-line to the second on top of the TURN-surface becomes visible. This TURN-surface can be used to normalize the urban area from this initial temperature drift for building insulation investigation.

4.3. Variation of Interpolation Parameters

The IDW interpolation of the deviation values, which results in the TURN-surface, can be influenced by several parameters. Here we want to highlight the interpolation radius and the smoothing factor, by comparing the visual appearance, resulting RMSE and temperature behaviour at our 18 reference points along road "Richard-Wagner Strasse". For this comparison we are using T_{gmean} and the tile size of 15x15 m.

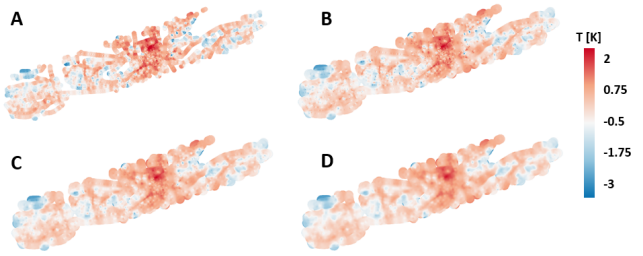

Figure 3: *TURN-surfaces calculated with T_{gmean} and various interpolation parameters.*

Figure 3 shows in **A** the TURN-surface with an interpolation radius of 50 m and in **B** an interpolation radius of 100 m. In either case, a smoothing factor of zero was chosen. Figure 3 **C** and **D** both have an interpolation radius of 100 m with an additional smoothing factor of 10 and 20.
Visually, the influence of the radius and the smoothing is quickly apparent. Figure 3 **A** appears patchy and the roads are partially recognizable, as interpolation is performed over a shorter distance. With a radius of 100 m, the TURN surface is almost filled, but without smoothing it has large fluctuations at certain points. Figure 4 shows that the resulting RMSE (across all flight-lines) changes for the different parameter configurations. Here it becomes clear that the configurations without smoothing deliver the best results.

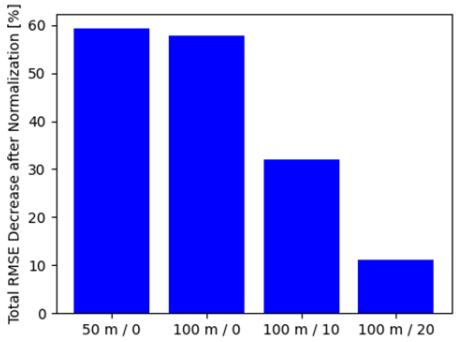

Figure 4: *RMSE decrease after normalization for various parameter configurations.*

The influence of smoothing is also well illustrated by Figure 5, showing the effect of parameter configurations on the 18 ground measurement points along the reference road. Each point has been buffered and averaged by a circle of 1.5 m radius, with point 1 being the northernmost on the road. Here it can be seen that the two configurations without smoothing have very similar temperatures and the higher the smoothing factor, the flatter the temperature of the TURN surface becomes. Extremely strong smoothing would lead to a completely flat curve. Based on this data, we decided to carry out the comparison with the reference measurements using the 100 m/0 configuration.

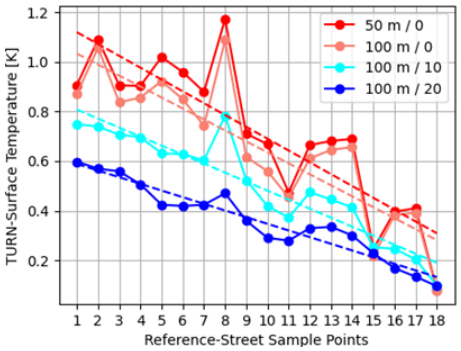

Figure 5: *TURN-surface temperatures at the reference-street sample points for the various interpolation parameters.*

4.4. Validation through Reference Measurements

It remains to be confirmed that the calculated TURN-surfaces indicate actual heat and cold islands. The pronounced heat island in the city center seems plausible, but we wanted to know whether the interpolated TURN-surface can also be applied to smaller neighborhood roads. For this purpose, the reference road ("Richard-Wagner-Strasse") was measured three times during one hour at 18 ground

points with a handheld infrared camera and the temperature values were averaged. These averaged temperature values are shown in Figure 6, together with the TURN-surfaces with T_{gmean} and $\overline{T}_{gmean}$. The reference values are displayed as *absolute* temperatures in K.

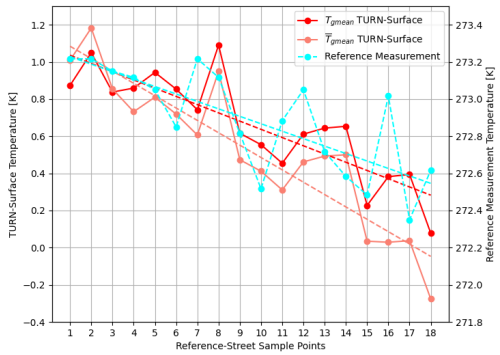

Figure 6: *TURN-Surface temperatures calculated with $\overline{T}_{gmean}$ and T_{gmean} together with the reference measurements at the street sample points.*

It can be seen that both the reference measurement and the TURN-surfaces show a cooling of the road in southern direction with a similar temperature delta. The graph shows that the $\overline{T}_{gmean}$ TURN-surface has a steeper temperature drop than the T_{gmean}-surface. This could be explained by the fact that the reference road points are mainly located in the third flight-line and only few points are located in the second and fourth flight-line. The $\overline{T}_{gmean}$ TURN-surface shows a mix of temporal and microclimatic characteristics with $\overline{T}_{gmean}$ being near the points 15, 16 and 17. An open question remains as to whether the averaged reference measurements should be compared with the $\overline{T}_{gmean}$ or the T_{gmean} surface. We take the view that the averaging of the reference measurements taken at three times during the flight removes the temporal aspect to some extent and therefore the T_{gmean}-surface represents the better comparison.

Furthermore, the normalization can be examined by comparing the TIR-image with the reference measurements. In Figure 7 the input temperature of the 1 m TIR-mosaic and the normalized temperatures on the 0.25 m TIR, calculated with T_{gmean}, is shown together with the original reference measurement. In this graph, the effect of normalization is clearly shown by the trend line, as it flattens out compared to the TIR. It can also be seen that the reference temperature from the handheld IR-device deviates from the TIR, because the infrared measurement was not corrected.
The TIR-mosaic temperature correction was supported by the two asphalt temperatures that were measured with iButtons. One iButton reference measurement was located at approx. point 5 and showed a temperature of 275.08 K during the overflight. The second iButton located near street "Weilerstrasse" measured a temperature of 273.15 K during the overflight (see supplementary material). The comparison of the TURN-surface at the location of the iButtons shows a temperature difference of 1.3 K and a cold island

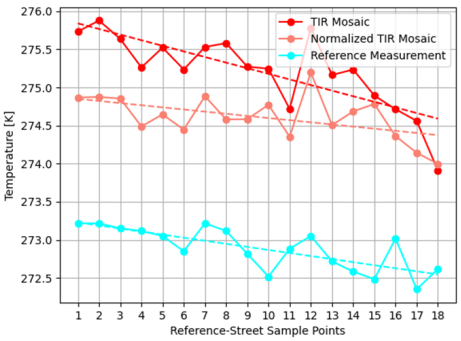

Figure 7: *Absolute temperatures of the TIR-mosaic before and after normalization, together with the reference measurement at the reference sample points.*

around "Weilerstrasse". Although there is a deviation, the trend is clearly correct and this comparison further supports the calculated results.

4.5. Correlation Analysis of TURN-Surface

The urban microclimate is influenced by many natural and man-made factors. While a higher density of streets and buildings causes warming, green spaces and open terrain are responsible for cooling [BSK20]. We therefore wanted to validate our calculated TURN-surfaces by means of correlation. We expected that the building area would be positively correlated with the TURN-surface and that the sky-view factor, which cools an area when close to a value of 1, would be negatively correlated. After evaluating the correlation matrix, our assumptions were confirmed. The building area is rather strongly correlated with increased temperatures and the sky-view factor raster has a slight but convincingly negative correlation with the TURN-surface (see supplementary material). This further confirms that the algorithm delivers mostly reliable results.

4.6. Conclusions and Outlook

In this work, a TIR-mosaic of the city of Aalen (Germany) was processed using the TURN algorithm for two reasons: First, to analyse the microclimate variability across the scene with the help of the TURN-surface and second, to clean the TIR-mosaic from microclimatic impacts for building insulation investigation, i.e. by normalizing it. The TURN algorithm was originally developed by [RHCH14] and adapted here to the encountered circumstances. A key difference to the original study is that our flight perimeter covered adjacent flight-lines. The relevant resulting temperature points from the algorithm thus had to be interpolated between flight-lines to create a perimeter-wide result.
We conclude from this study that special care must be taken to ensure that the most "road-like" temperature is calculated correctly for adjacent flight-lines (see 4.1). Instead of the *mode* value, we used the *geometric mean* to calculate the most "road-like" temperature, as this calculation method has an averaging character and outliers in the data have less influence on the result when compared to

the arithmetic mean. Considering flight-lines individually and later on interpolating them has the advantage of producing very clear microclimate-maps or TURN-surfaces (4.3).
However, this method is only suitable to a limited extent for normalizing the TIR-mosaic if one aims to e.g. compare the temperature of buildings across the full perimeter. A decisive factor here is the potential temperature drift during the recording of the data with remote sensing aircraft. If one looks at the flight-lines individually and then interpolates them, the potential temperature drift is not apparent. One solution, which includes the temporal temperature drift to some extent, is to define a *global* most "road-like" temperature across all flight lines. In this way, the temperature drift is also included to a large extent in the subsequently normalized TIR-mosaic.
The TURN algorithm aims at efficiently extracting and processing road temperatures. In this work, we validated the resulting microclimate-raster with various ground measurements on roads and thus created confidence in the calculated data (4.4). However, we have only shown that (i) the measured TIR shows correct temperatures and (ii) the TURN algorithm extracts and processes the temperatures correctly. With visual analysis and correlation investigation to the surface model and the building area, we were able to show that the calculated microclimate is plausible to a large extent. However, it remains questionable whether the measured street temperatures actually correspond to the microclimate in every scenario. For an extensive validation of the method, a large-scale temperature measurement network would have to collect data on the ambient and street temperatures, which would then have to be compared with the TURN-surface. Overall, TIR recordings via remote sensing aircraft offer great potential - not only to examine building envelopes and insulation standards, but also as a tool to detect heat and cold islands and to improve the well-being of people in cities with targeted actions.

5. Acknowledgements

This work was funded by Innosuisse (Grant No. 52958.1 IP-EE). TIR-data presented in this publication was acquired by BSF Swissphoto. The authors would like to thank BSF Swissphoto and Considerate AG for their support and effort in this project. Dario Jaeggi is thanked for the processing of auxiliary data used in this work.

References

[BMG19] BITELLI G., MANDANICI E., GIRELLI V. A.: Multi-scale remote sensed thermal mapping of urban environments: Approaches and issues. In *International Workshop on R3 in Geomatics: Research, Results and Review* (2019), Springer, pp. 375–386. 1, 2, 3

[BSK20] BHERWANI H., SINGH A., KUMAR R.: Assessment methods of urban microclimate and its parameters: A critical review to take the research from lab to land. *Urban Climate 34* (2020), 100690. URL: https://www.sciencedirect.com/science/article/pii/S2212095520302364, doi:https://doi.org/10.1016/j.uclim.2020.100690. 7

[GCK17] GULBE L., CAUNE V., KORATS G.: Urban area thermal monitoring: Liepaja case study using satellite and aerial thermal data. *International journal of applied earth observation and geoinformation 63* (2017), 45–54. 1

[GDA] GDAL/OGR CONTRIBUTORS: GDAL/OGR geospatial data abstraction software library. https://gdal.org GDAL/OGR 3.7.1 release (Feb. 2024). 4

[Jen09] JENSEN J. R.: *Remote sensing of the environment: An earth resource perspective 2/e*. Pearson Education India, 2009. 2

[MC16] MANDANICI E., CONTE P.: Aerial thermography for energy efficiency of buildings: the chot project. In *Remote Sensing Technologies and Applications in Urban Environments* (2016), vol. 10008, SPIE, pp. 57–65. 3

[MDH*21] MACLEAN I. M., DUFFY J. P., HAESEN S., GOVAERT S., DE FRENNE P., VANNESTE T., LENOIR J., LEMBRECHTS J. J., RHODES M. W., VAN MEERBEEK K.: On the measurement of microclimate. *Methods in Ecology and Evolution 12*, 8 (2021), 1397–1410. 2

[NAS] NASA: ECOSTRESS Spectral Library v.1.0. https://speclib.jpl.nasa.gov/ (Feb. 2024). 3

[RHCH14] RAHMAN M. M., HAY G. J., COULOIGNER I., HEMACHANDRAN B.: Transforming image-objects into multiscale fields: A geobia approach to mitigate urban microclimatic variability within h-res thermal infrared airborne flight-lines. *Remote Sensing 6*, 10 (2014), 9435–9457. 1, 2, 3, 4, 5, 7

[SPE] SPECTRAL SCIENCES INC.: MODTRAN Demo. http:///modtran.spectral.com/modtran$_{h}ome(Feb.2024)$. 3

[SSP*21] SMITH P., SARRICOLEA P., PERALTA O., AGUILA J. P., THOMAS F.: Study of the urban microclimate using thermal uav. the case of the mid-sized cities of arica (arid) and curicó (mediterranean), chile. *Building and Environment 206* (2021), 108372. 1

[YYZ20] YANG C., YAN F., ZHANG S.: Comparison of land surface and air temperatures for quantifying summer and winter urban heat island in a snow climate city. *Journal of Environmental Management 265* (2020), 110563. URL: https://www.sciencedirect.com/science/article/pii/S0301479720304965, doi:https://doi.org/10.1016/j.jenvman.2020.110563. 5

[ZXB*18] ZHOU D., XIAO J., BONAFONI S., BERGER C., DEILAMI K., ZHOU Y., FROLKING S., YAO R., QIAO Z., SOBRINO J. A.: Satellite remote sensing of surface urban heat islands: Progress, challenges, and perspectives. *Remote Sensing 11*, 1 (2018), 48. 1